

## RADIAL VELOCITY STUDY OF UZ SERPENTIS

Juan Echevarría<sup>1</sup> and Raúl Michel<sup>2</sup>

Received 2007 January 15; accepted 2007 April 10

### RESUMEN

Se presentan observaciones de alta dispersión espectral y resolución temporal de la nava enana UZ Ser. Encontramos la curva de velocidad radial del disco de acreción, alrededor de la estrella primaria, con una semi-amplitud  $K_1 = 98 \text{ km s}^{-1}$ . No se detecta evidencia de la estrella secundaria. El período orbital, estimado de esta curva de velocidad, es de 0.17589 días, ligeramente mayor al encontrado por Echevarría (1988) a través de observaciones fotométricas. Se discuten nuevas efemérides del objeto, basadas en ambos resultados. Un análisis de las masas y el ángulo de inclinación de la binaria, utilizando el diagrama de diagnóstico de masas  $M_1$ - $M_2$ , favorece un conjunto de valores para  $M_1 = 0.90 \pm 0.1M_\odot$ ;  $M_2 = 0.40 \pm 0.1M_\odot$ ;  $i = 50^\circ \pm 0.1$ , consistentes con las observaciones y modelos en el ultravioleta y la fotometría óptica.

### ABSTRACT

We present high dispersion time-resolved spectroscopic observations of the dwarf nova UZ Ser. We find the radial velocity curve of the accretion disc, surrounding the primary star, with a semi-amplitude  $K_1 = 98 \text{ km s}^{-1}$ . There is no spectral evidence of the secondary star. The orbital period, estimated from its velocity curve is 0.17589 days, slightly larger than that found by Echevarría (1988), from photometric observations. New ephemerides of the object are discussed from both results. An analysis of the masses and inclination angle of the binary, using the diagnostic  $M_1$ - $M_2$  diagram, favors a set of values with  $M_1 = 0.90 \pm 0.1M_\odot$ ;  $M_2 = 0.40 \pm 0.1M_\odot$ ; and  $i = 50^\circ \pm 0.1$ , which is consistent with the ultraviolet observations and models and also with the optical photometry.

**Key Words:** BINARIES: CLOSE — STARS: DWARF NOVAE — STARS: INDIVIDUAL (UZ SERPENTIS)

### 1. INTRODUCTION

UZ Serpentis is a dwarf nova, first identified by Petit (1960) as a U Gem star. There is some evidence that the star might be a Z Cam star (Dick 1987, 1989), but the light curve shown by the AAVSO during the last 10 years (see [www.aavso.org](http://www.aavso.org)), show that the star spends most of its time at a high state, at a magnitude  $V \approx 13$ , with occasional erratic low states between 15–17 mag, which suggests the possibility of an anti-dwarf nova classification. The ultraviolet and optical flux distribution have been thoroughly observed by Panek (1979), Echevarría et al. (1981) and Verbunt et al. (1984), both at high and low states. Photometric observations during a

low state ( $V \approx 16$  mag) have led to the discovery of the orbital period by Echevarría (1988). The system shows a periodic modulation which the author attributes to a hot spot being obscured by the accretion disc rather than to ellipsoidal variations of the secondary. Lake & Sion (2001) have fitted high-gravity atmosphere and accretion disc models to a far-UV spectrum of UZ Ser at a low state. They find that the spectrum is best fitted with  $\log g = 8$ ,  $T_{\text{eff}} = 27,000 \text{ K}$  for solar abundances, and a best accretion disc fit for  $M_1 = 1.0M_\odot$ , and disc inclination  $i = 75^\circ$ . In this paper we present the first radial velocity study of this binary and discuss the results with respect to the previous studies.

### 2. OBSERVATIONS

UZ Serpentis was observed in 2002 June 19 and 20 with the Echelle spectrograph at the f/7.5

<sup>1</sup>Instituto de Astronomía, Universidad Nacional Autónoma de México, México, D. F., México.

<sup>2</sup>Instituto de Astronomía, Universidad Nacional Autónoma de México, Ensenada, B. C., México.

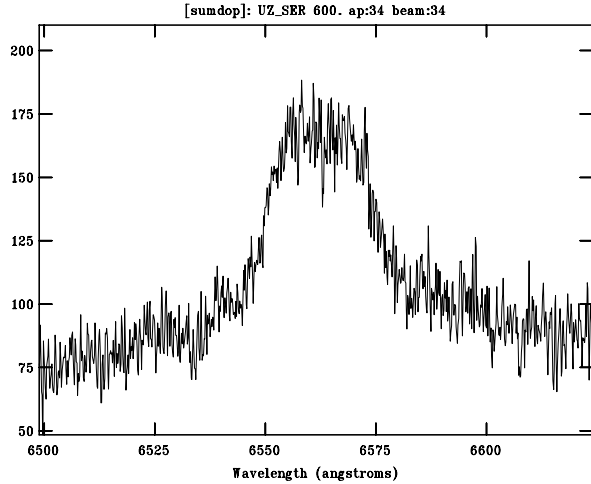


Fig. 1. Co-added spectrum of the H $\alpha$  emission line (see Section 3.2 for a full description).

Cassegrain focus of the 2.1-m telescope of the Observatorio Astrónomico Nacional at San Pedro Mártir, B. C., México. The Thompson 2048 $\times$ 2048 CCD was used to cover a spectral range from  $\lambda$ 3600 to  $\lambda$ 7100 Å with a spectral resolution of  $R=18,000$ . An echelle grating of 300 l/mm was used. The main feature of the spectra is a weak H $\alpha$  emission line. A very narrow and also weak nebular emission –which probably comes from the surroundings in this extremely patchy and reddened region (Echevarría et al. 1981)– was detected and subtracted. No absorption features were detected from the secondary star. The exposure time during the first night was 900 s and 1200 s during the second night. A co-added spectrum of the H $\alpha$  line (see Section 3.2) is shown in Figure 1. The data reduction was carried out with the IRAF package<sup>3</sup>. Simultaneous CCD photometry was obtained during the same nights using the 0.84-m Telescope and the SITe1 detector with a V filter. The integration time was 120 s. A nearby comparison star with  $V = 15.43$  mag was used to derive the magnitude of UZ Ser. The magnitude of the comparison star was derived from the comparison star observed by Echevarría et al. (1981).

### 3. RESULTS

#### 3.1. V Photometry

The light curves for the object and the comparison star are shown for both nights in Figure 2.

<sup>3</sup>IRAF is distributed by the National Optical Observatories, operated by the Association of Universities for Research in Astronomy, Inc., under cooperative agreement with the National Science Foundation.

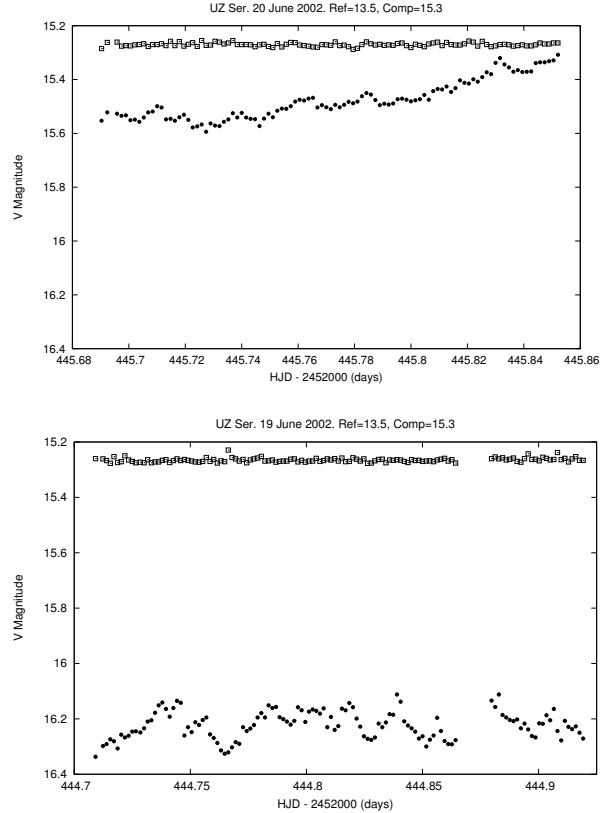


Fig. 2. Light curves of UZ Ser and the comparison star, obtained simultaneously with the spectroscopic data.

The observations were obtained during a short-lived low state, as shown by our observations and by the AAVSO data (see [www.aavso.org](http://www.aavso.org)). They have only one validated point with  $V \approx 16$  in their light curve, while 6 days before and 12 days after, the system appears at a high state with  $V \approx 13$ . Figure 2 (bottom) shows that during the first night the system varies with an amplitude of 0.2 mag, but remains at a mean magnitude around 16 during the 5 hr run. At the beginning of the second night (Figure 2 top), UZ Ser is already brighter with  $V \approx 15.35$  and continues to rise during the night, reaching 15.1 mag, with very small amplitude variations during the 4 hr run. We do not detect the orbital modulation observed by Echevarría (1988).

#### 3.2. Radial Velocity Diagnostic Diagram for H $\alpha$

The H $\alpha$  emission line was measured using the standard double Gaussian technique and its diagnostic diagrams as described in Shafter, Szkody, & Thorstensen (1986).

We refer to this paper for the details on the interpretation of our results. We have used the *con-*

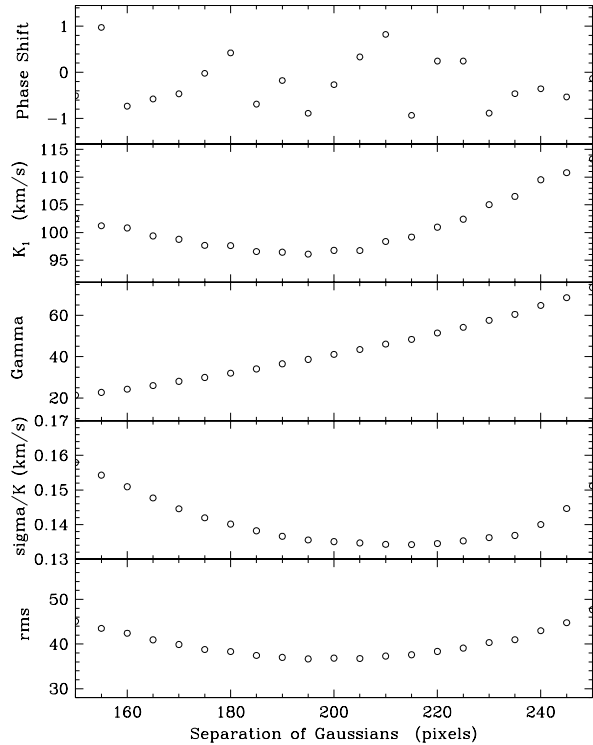


Fig. 3. Diagnostic Diagram. The best estimate of the semi-amplitude of the white dwarf is  $98 \text{ km s}^{-1}$ , corresponding to  $a \approx 210$  pixels.

olve routine from the IRAF *rvsao* package, kindly shared with us by Thorstensen (private communication). We have fixed the width of the Gaussians to 50 pixels and ran the double-Gaussian program for a range of separations  $a$  from 150 to 250 pixels. The results obtained are shown in Figure 3.

If low velocity asymmetric components are present, the phase shift should give spurious results for low values of  $a$ , and then should get steadier; in our case, due to the low signal to noise ratio of the observed line, the phase shift varies randomly for all tested values of  $a$ . The systemic velocity increases smoothly and reaches a maximum of about  $75 \text{ km s}^{-1}$  for the maximum Gaussian separation of 250 pixels. The semi-amplitude also decreases asymptotically as  $a$  increases until  $K_1$  approaches the correct value. On the other hand, as expected, the  $\sigma(K)/K$  vs  $a$  curve has a change in slope, at a value of  $a = 215$  when the individual Gaussians have reached the velocity width of the line at the continuum. For larger values of  $a$  the velocity measurements become dominated by noise. In our case, we have also plotted the rms value, which behaves similarly to the  $\sigma(K)/K$  ratio, but changes in slope

TABLE 1  
MEASURED  $\text{H}\alpha$  RADIAL VELOCITIES

HJD (240000+)	$\text{H}\alpha$ ( $\text{km s}^{-1}$ )
52444.70795	-24.198
52444.71763	21.279
52444.72730	27.702
52444.73941	72.095
52444.75256	138.830
52444.76568	91.448
52444.78263	98.886
52444.79578	60.585
52444.80891	140.409
52444.82780	-0.308
52444.84094	-80.978
52444.85408	-111.539
52444.87802	30.327
52444.89116	26.536
52444.90432	51.101
52445.75787	8.757
52445.77449	39.633
52445.79111	73.987
52445.80773	127.099
52445.82435	160.150
52445.84097	198.939

here at a slightly different value of  $a = 205$ . We believe the difference is again due to the low signal to noise ratio of the observations. Since the  $K$  velocity does not change substantially between these values we take a mean value  $a = 210$  pixels as the best value, corresponding to  $K_1 = 98 \text{ km s}^{-1}$ .

The radial velocities corresponding to the adopted solution are shown in Table 1, while the corresponding orbital parameters obtained from our nonlinear least-squares fit program are given in Table 2. The radial velocities are also plotted in Figure 4. Open circles correspond to velocity measurements from the first night, while filled dots represent data from the second night. The solid line close to the points corresponds to a sinusoid fit with the parameters presented in Table 2. We can see from the orbital phase distribution of the points that not enough data were obtained from phase 0.9 to phase 0.3. We searched for a possible alias period with our program, but found no satisfactory solution for periods of up to 0.5 days. This is particularly important,

TABLE 2  
ORBITAL PARAMETERS DERIVED FROM  
THE WINGS THE  $\text{H}\alpha$  EMISSION LINE

Orbital Parameters	$\text{H}\alpha$
$\gamma$ (km s $^{-1}$ )	46 $\pm$ 9
$K$ (km s $^{-1}$ )	98 $\pm$ 13
HJD $_{\odot}$	0.8224 $\pm$ 0.19
(+2446622 days)	
$P_{\text{orb}}$ (days)	0.17589(2)
$\sigma$	37.3

in order to discard the possibility that the photometric modulations found by Echevarría (1988) are due to ellipsoidal variations of the secondary. Echevarría (1988) also points out that, in such a case, the orbital period should be above 8 hr and consequently the spectrum of the secondary should be well detected, which our spectral observations do not support. The sinusoidal variation of the  $\text{H}\alpha$  line is consistent with the motion of the accretion disc surrounding the primary star. Moreover, the broad shape of the emission line is consistent with a typical emission line produced by an accretion disc with a moderate inclination angle (Horne & Marsh 1986). To show this, we have plotted  $\text{H}\alpha$  in Figure 1. Since our individual spectra have a very low signal to noise ratio, we have constructed a mean spectrum by co-adding the individual spectra in the frame of reference of the disc - white dwarf. The spectra have been Doppler-corrected by a sinusoidal fit using the orbital parameters derived in this section. By this process, we avoid a smearing of the emission line due to the radial velocity variations and allow the mean shape to be seen with a maximum signal to noise ratio. The wings of the lines extend to about 1000 km s $^{-1}$ , typical of orbiting material at large radii. The peak of the line seems a little broader for a single line profile and there is also a very narrow absorption in the middle, supporting the idea of an overlapped double profile. However, we believe that spectra with better signal to noise ratio and phase coverage should be obtained, before reaching any conclusion about a double-peak profile, as this point might be crucial for setting limits to the inclination angle of the binary. More observations are also needed to better evaluate whether or not the disc follows the dynamical motion of the primary star.

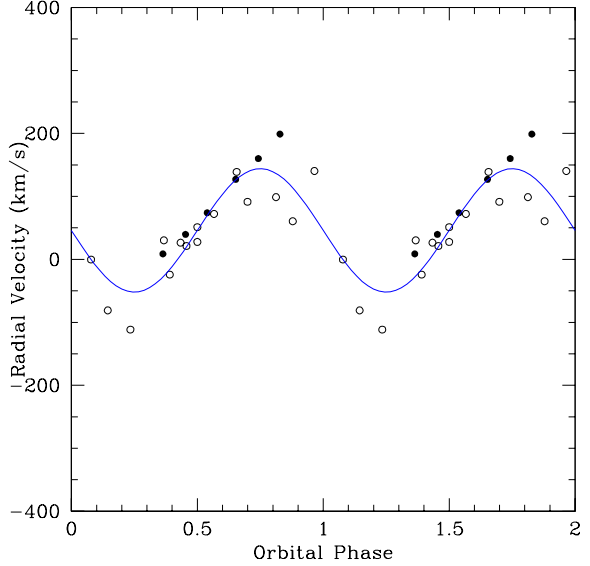


Fig. 4. Radial velocities UZ Ser. Open circles shows data from the first night and dots from the second night. The solid line is the best fit.

### 3.3. Improved Ephemerides of UZ Ser

The photometric results by Echevarría (1988) give an ephemeris of HJD=2446622.6536+0.1730E (corrected by heliocentric motion), and they correspond to the point of minimum light. One orbital period later (0.1730) the zero point is 244,662.8266. Comparing this zero point with that in Table 2 we see that there is a difference of 0.01 in orbital phase between both results, a value which is within the errors. The fact that the zero point of the radial velocity curve corresponds to the orbital phase when the primary is in front of the secondary supports the explanation that the photometric variations are due to the obscuration of a bright spot by the disc itself. If this is so, then we can combine both the photometric and the spectroscopic results to give an improved ephemeris:

$$\text{HJD} = 2446622.68149(5) + 0.17589(2) \text{ E} ,$$

for the inferior conjunction of the secondary star. This ephemeris will be used hereinafter.

### 3.4. The $M_1$ - $M_2$ Diagnostic Diagram

Adopting the 0.17589 day orbital period from the  $\text{H}\alpha$  line solution, and taking  $K_1=K_{\text{em}}=98$  km s $^{-1}$  we can use the  $M_1$ - $M_2$  Diagnostic Diagram by Echevarría et al. (2007) to obtain mass and inclination angle estimates for this system. This is shown in Figure 5 for three mass ratios:  $q = 0.3$ ,

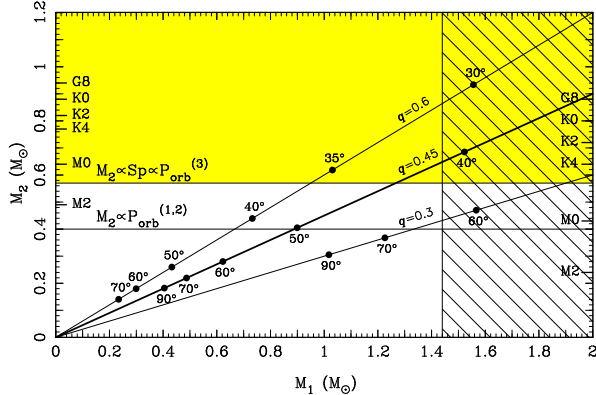


Fig. 5.  $M_1 - M_2$  diagram (see text for explanation).

0.45 and 0.6. In this diagram the mass ratios are simple straight lines which, for a given value of  $M_1$ , have a corresponding value of  $M_2$ . They do not depend on any other assumption or on observed values like  $K_1$ ,  $K_2$ , or  $P_{orb}$ . The vertical line lies at the Chandrasekhar limit and divides the white dwarf and neutron star degenerate regimes. The horizontal thin lines give the value of  $M_2$  from the empirical  $M_2$ - $P_{orb}$  relations by Echevarría (1983; Label 1) and Warner (1995, page 111; Label 2). These two relations using the improved orbital period give  $M_2 = 0.40 M_\odot$  and  $M_2 = 0.39 M_\odot$ , respectively. The horizontal upper region (shown in gray) is limited by the value obtained from the  $M_2$ - $Sp$  and  $Sp$ - $P_{orb}$  relations in Kolb & Baraffe (2000) for ZAMS secondaries (see their Figures 1 and 3), which, for our orbital period give an M1 spectral type and  $M_2 = 0.57 M_\odot$  (Label 3). The spectral types labeled on the left side of the diagram correspond to the ZAMS stars models discussed by Kolb & Baraffe (2000). These spectral types, their corresponding masses for the secondary, and the upper mass limits for both stars in the binary, are specific constraints, namely, that the primary star cannot exceed the Chandrasekhar limit, and that the secondary star lies on the ZAMS. Cataclysmic variables probably do not contain normal main sequence stars (e.g. Echevarría 1983; Beuermann et al. 1998). However, as pointed out by these authors, for short orbital periods, as in the case of UZ Ser, the secondary stars are closer to the main sequence than are systems with larger orbital periods. If the secondary stars are in an evolved sequence with constant  $M$ , but with a fraction  $X_c$  still burning in its core, then the spectral type for a given mass will be later than that of a ZAMS star (see Figures 1 and 2 in Kolb & Baraffe 2000 for extreme assumptions). Therefore, the whole spectral type scale in

the diagram will go down, as shown on the right side of the diagram.

The inclination angle of the binary can be found from the mass function:

$$M_{1,2} \sin^3 i = 1.036 \times 10^{-7} P_{orb} K_{2,1} (K_1 + K_2)^2 M_\odot,$$

where  $P_{orb}$  is given in days and  $K_{2,1}$  in  $\text{km s}^{-1}$ . It is straightforward to see that knowledge from two of these variables will yield the inclination angle (for a given  $q$ ) as a function of  $M_1$  or  $M_2$ . Since we know  $P_{orb}$  and  $K_1$  we can derive values of  $i$  along the  $q$  lines. Some selected values of  $i$  are shown as dots in the  $M_1$ - $M_2$  diagram.

We can now use this diagnostic diagram to find consistent values of  $M_1$ ,  $M_2$  and  $i$ . Since the binary is not an eclipsing system we can assume that  $i$  is less than about  $70^\circ$ . We also have two possible constraints; one is the mass of the secondary star  $M_2 = 0.40 M_\odot$  (see discussion above); the other, a possible combination of  $M_1 = 1.0 M_\odot$  and  $i = 75^\circ$  from Lake & Sion (2001). On the other hand a  $q$  value of 0.3 seems unlikely as the white dwarf would have to be a very massive star. Still it is possible, if take  $M_2 = 0.40 M_\odot$  at face value, which gives  $M_1 = 1.34 M_\odot$  and  $i$  about  $65^\circ$ . For  $q = 0.6$  the system would have to have low masses, since low values of  $i$  would not be consistent with optical modulations with an amplitude of 0.26 mag (Echevarría 1988). A  $q$  value of 0.45 seems more likely. For this mass ratio we have a set of values  $M_1 = 0.90 \pm M_\odot$ ;  $M_2 = 0.40 M_\odot$  and  $i = 50^\circ$ , which is compatible with the ultraviolet and optical constraints. The uncertainties in the masses and the inclination angle are difficult to evaluate at this point, but, for a possible value of  $q$  of 0.45, the errors should not be much greater than 0.1. Further observations are required, however, especially a near-infrared radial velocity study of the secondary, in order to obtain  $K_2$  directly from observations, to check on the assumptions we have made in this paper, and to obtain accurate masses and a reliable inclination angle of the binary. Since UZ Ser is highly variable and its classification is uncertain, it would be advisable to conduct simultaneous spectroscopy and photometry, during a larger time-span.

#### 4. CONCLUSIONS

Our main conclusions are as follows.

- (1) We obtained a high resolution time-resolved spectroscopy of UZ Ser. We detected the presence of weak  $\text{H}\alpha$  in emission and no evident signature

from the secondary star. Simultaneous photometry showed that the system was at a non-stable low state.

(2) A radial velocity amplitude of  $98 \text{ km s}^{-1}$  was obtained from the accretion disc producing this emission and an orbital period of  $0.17589 \text{ d}$  was found from the radial velocity analysis. Comparing this with the photometric data taken 16 years before, we improved the ephemerides of the system.

(3) An analysis of the masses and inclination angle of the binary, using the diagnostic  $M_1$ - $M_2$  diagram favors a set of values  $M_1 = 0.90M_\odot$ ;  $M_2 = 0.40M_\odot$  and  $i = 50^\circ$ , which is compatible with the ultraviolet and optical constraints.

(4) A near-infrared radial velocity study of the secondary star with simultaneous photometry is strongly recommended, in order to obtain accurate parameters of the binary.

I would like to thank the staff of the San Pedro Mártir Observatory for their support.

## REFERENCES

Beuermann, K., Baraffe, I., Kolb, U., & Weichhold, M. 1998, A&A, 339, 518

Dick, G. P. 1987, Jour. Am. Ass. Variable Star Obs., 16, 91

\_\_\_\_\_. 1989, Jour. Am. Ass. Variable Star Obs., 18, 105

Echevarría, J. 1983, RevMexAA, 8 109

\_\_\_\_\_. 1988, RevMexAA, 16, 37

Echevarría, J., Jones, D. H. P., Wallis, R. E., Mayo, S. K., Hassall, B. J. M., Pringle, J. E., & Whelan, J. A. J. 1981, MNRAS, 197, 565

Echevarría, J., Michel, R., Costero, R., & Zharikov, S. 2007, A&A, 462, 1069

Kolb, U., & Baraffe, I. 2000, NewA Rev., 44, 99

Lake, J., & Sion, E. M. 2001, AJ, 122, 1632

Horne, K., & Marsh, T. R. 1986, MNRAS, 218, 761

Panek, R. J. 1979, ApJ, 234, 1016

Petit, M. 1960, Jour. Observateurs, 43, 17

Shafter, A. W., Szkody, P., & Thorstensen, J. R. 1986, ApJ, 308, 765

Verbunt, F., et al. 1984, MNRAS, 210 197

Warner, B. 1995, Cataclysmic Variable Stars (Cambridge: Cambridge Univ. Press)

Juan Echevarría: Instituto de Astronomía, Universidad Nacional Autónoma de México, Apdo. Postal 70-264, México, 04510 D. F., México (jer@astrocu.unam.mx).

Raúl Michel: Instituto de Astronomía, Universidad Nacional Autónoma de México, Apdo. Postal 877, 22830 Ensenada, Baja California, México (rmm@astrosen.unam.mx).